Nature of mixed electrical transport in Ag_2O-ZnO-P_2O_5 glasses containing WO_3 and MoO_3

Luka Pavić,[a,*] Ana Šantić[a], Juraj Nikolić,[a] Petr Mošner,[b] Ladislav Koudelka,[b] Damir Pajić,[c] Andrea Moguš-Milanković[a]

[a]*Division of Materials Chemistry, Ruđer Bošković Institute, Bijenička 54, HR-10000 Zagreb, Croatia*
[b]*Department of General and Inorganic Chemistry, Faculty of Chemical Technology, University of Pardubice 53210 Pardubice, Czech Republic*
[c]*Department of Physics, Faculty of Science, University of Zagreb, Bijenička 32, HR-10000 Zagreb, Croatia*

Abstract

This study reports on the nature of electrical transport and role of structural changes induced by different type and content of TMO in Ag-containing glasses of xTMO-(30-0.5x)Ag_2O-(30-0.5x)ZnO-40P_2O_5 (TMO = MoO_3/WO_3, $0 \leq x \leq 60$ mol%) composition. Raman spectra show clustering of WO_6 units in glasses with high WO_3 content while the addition of MoO_3 induces a gradual change of MoO_6 octahedra to MoO_4 tetrahedra both being cross-linked with phosphate units without clustering. For WO_3 glasses, minimum in DC conductivity is observed at 30-40 mol% of WO_3 for temperatures from 303 to 513 K, followed by increase in conductivity with further WO_3 addition due to an increase in polaronic contribution. Observed turnover suggests a distinct transition from predominantly ionic to predominantly polaronic transport. Contrary, for MoO_3 glasses conductivity decreases in the whole mixed compositional range indicating the nature of transport is dominated by ionic component throughout the measured temperature range. A comparative study of Ag^+, Li^+, Na^+ transport in MoO_3/WO_3 glasses reveals strong correlation between pre-exponential factor and activation energy, which allows detection of the prevalence of conduction mechanism. Finally, the results demonstrate that Ag_2O-WO_3-ZnO-P_2O_5 glass system is a promising electrically tunable material with significant contributions of ionic or polaronic conductivity depending on composition.

Keywords: Mixed ion-polaron glasses, Transition metal oxide glasses, Impedance spectroscopy, Structure-property relationships, Cation mobility

*Corresponding author. Tel.:++385-1-4571-376
E-mail address: lpavic@irb.hr (Luka Pavić)

1. Introduction

In recent years, there has been a relentless pursuit for new types of materials which can replace the widely used traditional ones. The electrical transport in glasses has attracted much attention due to their potential use as electrolytes and electrode materials and boosted the ongoing search for new glassy materials [1-4]. Glasses containing silver ions are recognized as highly conductive electrolytes. This is especially true for glasses doped with silver chalcogenides or silver halides [5-12] where extremely high mobility of silver ions is achieved making these materials the fast ionic conductors with applications as solid electrolytes, in optical switches and memory devices. Moreover, an interesting applicative direction of these materials is their development in the solid state silver battery technology [13]. However, somehow limiting property of silver-rich glasses due to their hygroscopic nature is their relatively low glass transition temperature, typically less than 250 °C [7,14-16], which restricts the temperature range of the battery operation. On the other hand, oxide glasses where silver is introduced solely as Ag_2O [17-20] have higher T_g but the generally lower mobility of silver ions.

On the other hand, a wide compositional variability of oxide glasses offers a possibility to combine ionic conduction with electronic transport by the introduction of transition metal oxides (TMO) such as WO_3, MoO_3, V_2O_5 or Fe_2O_3. In addition to ionic contribution coming from cation movement through the glass network [21,22], the transition metal ions in these glasses exist in different oxidation states and the electron transport [23-25] takes place by polaron hopping between TMs. Such mixed conduction, although completely undesirable for the battery electrolyte, is highly important for the cathode materials in solid state batteries [26-28].

In Li-batteries, at high charge and discharge rates, there is a significant drop in battery capacity due to difficult movements of Li^+ ions and electrons in the mixed

cathode material. Effective movements of charge carriers should be quick enough through the material to utilize a large amount of charge in a short amount of time. In crystalline $LiFePO_4$ [29-31] based materials electronic and ionic conductivity each play a significant role in cathode performance. Low electronic conductivity observed in $LiFePO_4$ is crucial for performance at high current rates [29]. In the study by Wang et al. [30], it is shown how the rate performance of the balanced mixed electronic/ionic conductive $LiFe_{0.95}Mg_{0.05}PO_4$ is surprisingly higher than that of the electronic conductive $LiFe_{0.95}Ni_{0.05}PO_4$ and the ionic conductive $LiFePO_4$. The Li^+ ion diffusion is enhanced by the internal electrical field generated by the electrons. Moreover, interesting is that the electronic contribution in mixed conductor is lower than electronic conducting $LiFe_{0.95}Ni_{0.05}PO_4$. Several studies reported that best electrode performance is achieved when ionic transport is less than twice in magnitude than the polaronic one [29-32].

Glassy materials attract much attention due to their several advantages over crystalline counterparts such as isotropic conduction, no grain boundary effect, easy preparation, etc. In addition, the conductivity of glass is generally higher than that of corresponding crystalline ones because of their so-called open structure. While ionic and polaronic (electronic) conduction in oxide glasses separately have been well detailed, their dependence or independence seems to be in strong correlation with glass composition of the system under study [19,20,33-39]. Multiple papers have tried to explain the influence of various parameters on the conductivity of such systems but due to their complexity, the unambiguous answer has not been found. Among vast body of data, conductivity studies on mixed oxide glasses containing silver ions [19,20,34-36] have been receiving attention due to specific conductivity behavior in such systems. The role of silver cations in the mixed transport is different if compared

to the other monovalent cations probably due to different cation electronic configuration. In mixed conductive tellurite-based glasses [19,20,40] Ag^+ ions increase the DC conductivity by several orders of magnitude and decrease the activation energy in comparison to analogous with alkali ions instead. Such an unusual conductivity behavior indicates different nature of silver ions and additional interactions between charge carries and glass network and as such needs to be studied further and extended to similar glass systems.

In our most recent study, we investigated mixed conductive zinc-phosphate glass systems with WO_3/MoO_3 and Li_2O/Na_2O (TMO-M_2O-ZnO-P_2O_5) [41]. In both tungsten series containing lithium and sodium ions, a transition from ionic to polaronic electrical mechanism is evidenced by the presence of the conductivity minimum as alkali ions are replaced by WO_3. On the other hand, molybdenum series showed different behavior with almost constant DC conductivity suggesting an independent ionic and polaronic transport pathways.

In light of these facts, we present the extension of the mixed ion-polaron transport study on glass systems containing Ag_2O, namely xWO_3-(30-0.5x)Ag_2O-(30-0.5x)ZnO-40P_2O_5 and xMoO_3-(30-0.5x)Ag_2O-(30-0.5x)ZnO-40P_2O_5 ($0 \leq x \leq 60$ mol%). A special attention is paid to the predominance of each conduction mechanisms in correlation to the various parameters that are relevant for each of them including the structural properties of glasses. Moreover, this study seeks to address the role of cation in mixed conducting glasses and shed more light on the complexity of charge transfer nature. Thus we provide a comparative study of mobility of silver and alkali (Li^+ and Na^+) ions [41] in the zinc phosphate glasses containing MoO_3/WO_3 revealing the highest ionic conductivity of glasses containing significant amounts of silver ions and the huge contribution of polaronic conduction as Ag_2O is completely replaced by WO_3.

2. Experimental

2.1. Preparation of Glasses

Two series of glasses in the quaternary systems: xWO_3-(30-0.5x)Ag_2O-(30-0.5x)ZnO-40P_2O_5, labeled Ag-W and $xMoO_3$-(30-0.5x)Ag_2O-(30-0.5x)ZnO-40P_2O_5, labeled Ag-Mo with x = 0-60 (mol%) were prepared by conventional melt-quenching using an appropriate mixture of analytical grade $AgNO_3$, ZnO, H_3PO_4, and WO_3 or MoO_3. The experimental method of preparation used in this work is explained in details in Ref. 41 where similar glass compositions were prepared.

The volatilization losses checked by weighting were not significant, hence the batch compositions can be considered as reflecting actual compositions. The vitreous state of the samples was confirmed by X-ray diffraction. The composition of glasses studied in this paper is listed in Table 1.

Starting TMO-free glass, 30Ag_2O-30ZnO-40P_2O_5, is clear and transparent. The color of glasses change with the addition of WO_3 content and becomes intense blue, whereas glasses containing MoO_3 are of green color. Glass color intensifies as TMO content increases indicating an increase in the fraction of TM^{5+} ions, Table 1.

2.2. Density and Dilatometric Measurements

The glass density, ρ, was determined on bulk samples by the Archimedes' method using toluene as the immersion liquid. The molar volume, V_M, was calculated as $V_M = M/\rho$, where M is the average molar weight of the glass compositions aAg_2O-bZnO-cP_2O_5-dMoO_3 (or -WO_3), calculated for $a+b+c+d = 1$.

The thermal expansion of all prepared glasses was investigated by horizontal thermodilatometry using dilatometer DIL 402 PC (Netzsch). Dilatometric measurements were carried out on bulk samples with dimensions of 25×5×5 mm^3 in static air at the heating rate of 3 K min^{-1}. Obtained curves were evaluated by Proteus

software and values of glass transition temperature, T_g, dilatometric softening temperature, T_d and the thermal expansion coefficient, α, were determined, Table 1.

Table 1. Composition and experimental data for xTMO-(30-0.5x)Ag_2O-(30-0.5x)ZnO 40P_2O_5 (TMO = WO_3, MoO_3) series of glasses.

	WO_3	Ag_2O	ZnO	P_2O_5	T_g (K)	ρ (g cm^{-3})	V_m (cm^3 mol^{-1})	O/P	W/P	W^{5+}/W_{tot} (%)
Ag-0TMO	0	30	30	40	513	4.40	34.3	3.25	0	0
Ag-10W	10	25	25	40	557	4.41	35.9	3.50	0.125	-
Ag-20W	20	20	20	40	600	4.45	37.3	3.75	0.250	0.42
Ag-30W	30	15	15	40	651	4.42	39.3	4.00	0.375	0.51
Ag-40W	40	10	10	40	729	4.45	40.5	4.25	0.500	0.80
Ag-50W	50	5	5	40	800	4.44	42.4	4.50	0.625	1.00
40P-60W	60	0	0	40	793	4.41	44.4	4.75	0.750	1.45
	MoO_3	Ag_2O	ZnO	P_2O_5				O/P	Mo/P	Mo^{5+}/Mo_{tot} (%)
Ag-10Mo	10	25	25	40	543	4.15	36.1	3.50	0.125	2.88
Ag-20Mo	20	20	20	40	593	3.94	37.7	3.75	0.250	4.12
Ag-30Mo	30	15	15	40	649	3.72	39.5	4.00	0.375	5.71
Ag-40Mo	40	10	10	40	686	3.53	41.3	4.25	0.500	9.61
Ag-50Mo	50	5	5	40	714	3.33	43.4	4.50	0.625	15.07
40P-60Mo	60	0	0	40	751	3.15	45.4	4.75	0.750	37.04

2.3. Raman Spectroscopy

The Raman spectra of glasses were taken at room temperature on bulk samples using a Horiba-Jobin Yvon LaBRam HR spectrometer. The spectra were collected in back-scattering geometry under excitation with Nd-YAG laser radiation (532 nm) at a power of 12 mW on the sample. The spectral slit width was 1.5 cm^{-1} and the total integration time was 50 s. The complex shape of the experimentally obtained Raman spectra in the 200-1400 cm^{-1} range was analyzed using a least square fitting procedure assuming a Gaussian shape for all bands. The position and intensity of each component band were determined from the deconvoluted Raman spectra. The structural units in phosphate network were classified

according to their connectivity by Q^n notation where n represents the number of bridging oxygen atoms per PO_4 tetrahedron (n = 0-3).

2.4. Fraction of TM ions in different valance states

The fraction of molybdenum ions in different valence states, Mo^{5+}/Mo_{tot}, was determined using electron spin resonance (ESR) whereas, in case of tungsten ions, W^{5+}/W_{tot}, magnetization measurements using MPMS5 SQUID magnetometer were performed. Obtained values for TM^{5+}/TM_{total} fraction of TMO ions are given in Table 1 with errors less than 1%.

2.4.1. Electron Spin Resonance (ESR)

ESR spectra of powdered samples were recorded at ambient temperature on a spectrometer ESR 221 Magnettech Berlin operating at X-band microwave frequency (~ 9.5 GHz). Obtained spectra were double integrated and experimental parameters were used to obtain comparable areas of all spectra. The ratio of Mo^{5+}/Mo_{tot} was calculated from the obtained data using Mn^{2+} standard to determine the spin concentration in all measured glassy samples.

2.4.2. SQUID magnetometer

Temperature dependence of magnetization was measured from 2 K to 300 K in a constant magnetic field of 0.1 T. Due to unique sensitivity of the MPMS5 SQUID magnetometer it is possible to determine the small amount of the paramagnetic ions in studied glasses. To get the accurate results the measurements are performed with additional precaution needed to avoid any magnetic contamination as well as to maintain a constant temperature on the sample. Obtained data were analyzed using the Curie constant attributed to the isolated paramagnetic centers W^{5+} and the ratio of W^{5+}/W_{tot} was calculated for all prepared samples.

2.3. Impedance spectroscopy measurements

For the electrical measurements, annealed samples were prepared in form of ~1 mm thick disks and polished with SiC polishing paper. Gold electrodes, 6 mm in diameter, were sputtered onto both sides of disks using Sputter Coater SC7620 and stored in a desiccator until measurements. Electrical properties were obtained by measuring complex impedance using an impedance analyzer (Novocontrol Alpha-AN Dielectric Spectrometer) in a frequency range from 0.01 Hz to 1 MHz at temperatures between 303 and 513 K. The temperature was controlled to an accuracy of ± 0.2 K.

3. Results and discussion

3.1. General glass properties

Glass compositions along with the obtained values of physicals parameters such as glass densities, ρ, glass transition temperatures, T_g, and molar volumes, V_M, are listed in Table 1. Their dependence as a function of WO_3 and MoO_3 content, along with dilatation softening temperature, T_d, and thermal expansion coefficient, α, is shown in Fig. 1(a-d).

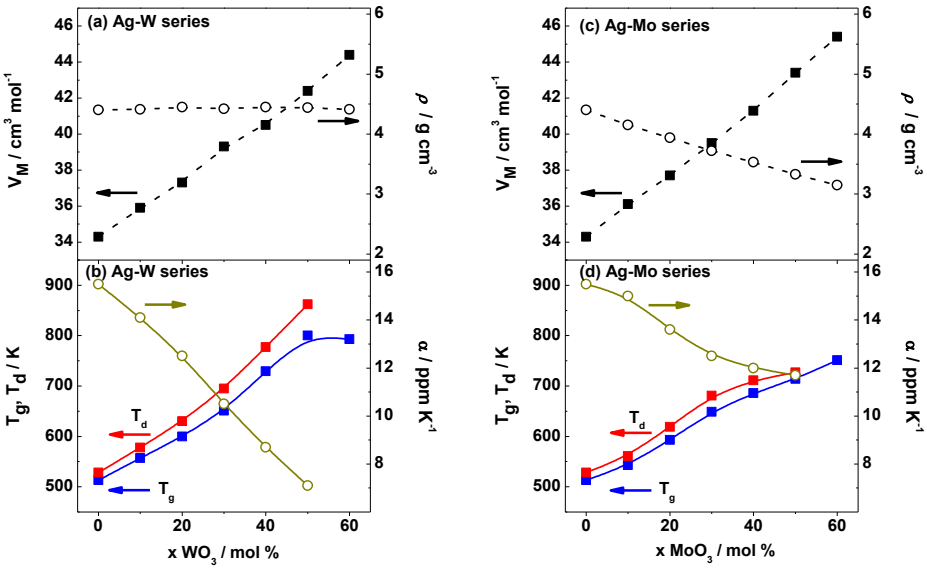

Fig. 1. Compositional dependence of the glass density, ρ, molar volume, V_M, glass transition temperature, T_g, dilatation softening temperature, T_d, and thermal expansion coefficient, α, for investigated series of glasses (a,b) Ag-W and (c,d) Ag-Mo.

It can be seen that V_M increases almost linearly for both series of glasses, from 34.3 to 44.4 cm^3 mol^{-1} for Ag-W and from 34.3 to 45.4 cm^3 mol^{-1} for Ag-Mo glasses as WO_3 and MoO_3 increases, Fig. 1(a,c). On the other hand, ρ decreases linearly in the entire compositional range for Ag-Mo glasses, in the range from 4.15 to 3.15 g cm^{-3}, whereas remains almost constant at ~4.4 g cm^{-3} for Ag-W series. Increase in molar volume and only slight changes in molar mass for Ag-Mo glasses are reflected in the observed decrease in glass density. On the contrary, for Ag-W glasses large mass difference between tungsten and silver atoms notably increases molar mass with WO_3 addition and in combination with a proportional increase in V_M have an impact on the constant value of glass density throughout Ag-W glass series.

Furthermore, the dependence of T_g, T_d, and α on WO_3 and MoO_3 content is shown in Fig. 1(b,d). From the results, it is evident that both T_g and T_d increase with increasing content

of transition metal oxide, with T_g increasing from 513 to 793 K for Ag-W and from 513 to 751 K for Ag-Mo glasses. However, a saturation in T_g is observed for Ag-W glass series at highest TMO content (50-60 mol%) which is not the case for Ag-Mo glasses. The systematic changes in thermal properties suggest the changes in the glass network with increasing WO_3 and MoO_3 content. Generally, glass transition temperature depends upon several factors such as the strength of chemical bonds, the degree of cross-linking of the network and density of packing of oxygen atoms [42]. The observed increase in T_g and T_d with increasing WO_3 and MoO_3 in these glasses reveals the formation of stronger bonding and cross-linking between phosphate and TM units which produces a compact glass network. It is worth mentioning that the values of T_g for Ag-W and Ag-Mo glasses are slightly higher than those determined for $NaPO_3$-WO_3 glasses [43] indicating a stronger bonding in the investigated glasses. Such behavior is attributed to the presence of ZnO which is responsible for the compactness of the glass network [41,44].

At the same time, the thermal expansion coefficient, α, continuously decreases through the whole compositional range with the addition of WO_3 as well as MoO_3 content, Fig. 1(c-d). However, the decrease is more pronounced for Ag-W glasses where it varies within the range of 15.0-7.1 ppm $°C^{-1}$ for 0-50 mol% WO_3 in comparison to an observed decrease in Mo-containing glasses within the range 15.0-11.7 ppm $°C^{-1}$ for 0-50 mol% MoO_3. This supports previous assumption that the glass structure strengthens with the addition of both TMOs, being slightly more pronounced in case of WO_3.

3.2. Structural Analysis

The structural modifications of silver zinc-phosphate glasses induced by addition of WO_3 or MoO_3 are shown in Raman spectra, Fig. 2 and 3. In order to obtain the precise position of the bands, Raman spectra of all investigated glasses were deconvoluted,

see Fig. 2(b-c) and 3(b-c). The assignment of the Raman bands according to the literature data is presented in Table 2.

Starting $30Ag_2O$-$30ZnO$-$40P_2O_5$ glass, free of TMO, shows polyphosphate structure characteristic for its compositional stoichiometry [41,45-48], bottom Raman spectrum in Figs. 2(a) and 3(a). This glass consists of dominant Q^2 and Q^1 phosphate units with barely detectable isolated Q^0 orthophosphate units, similarly as zinc phosphate glasses containing Li_2O and Na_2O [41].

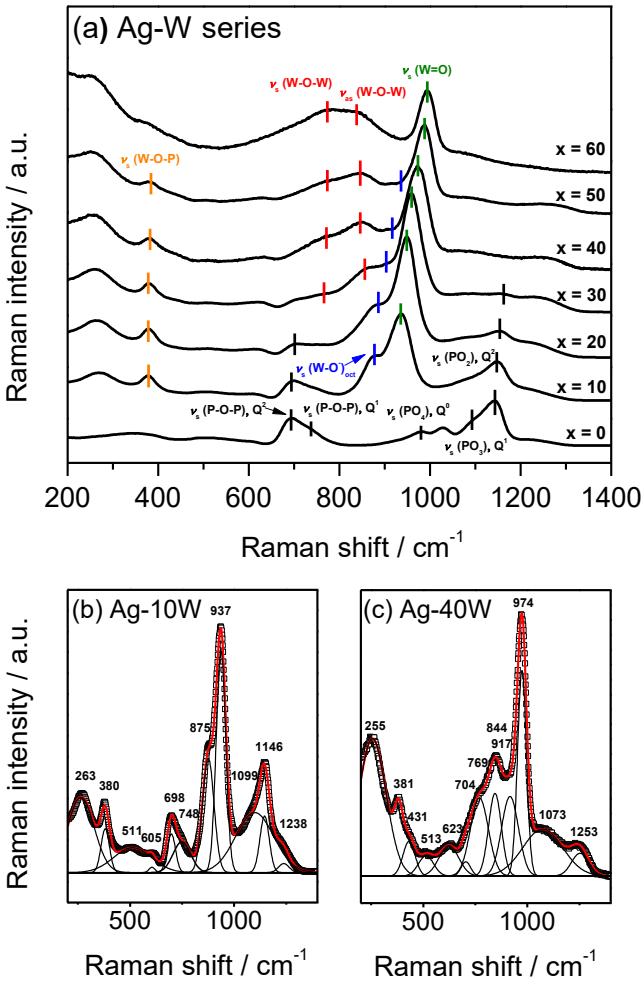

Fig. 2. (a) Raman spectra of xWO_3-$(30-0.5x)Ag_2O$-$(30-0.5x)ZnO$-$40P_2O_5$ series of glass and deconvolution of the Raman spectra for (b) Ag-10W and (c) Ag-40W in the 200-1400 cm^{-1} region.

In general, it is expected that addition of TMO into phosphate-based glass structure induces transformation of glass network during which depolymerization of metaphosphate and pyrophosphate chains occurs and WO_n and MoO_n polyhedra incorporate into phosphate structure.

Table 2. Raman bands and their assignment.

Wavenumber / cm^{-1}	Band	References
200-350	δ (O-W-O), δ (P-O)	41,45,46,49
380-390	ν_s (W-O-P)	41,43,49
390-400	ν_s (Mo-O-P)	41,50-52
450-650	δ (P-O)	41,45,46
690-735	ν_s (P-O-P) Q^2	41,45,46
730-770	ν_s (P-O-P) Q^1	41,45,46
760-785	ν_s (W-O-W), ν_s (Mo-O-Mo)	41,43,49-52
840-870	ν_{as} (W-O-W), ν_{as} (Mo-O-Mo)	41,43,49-52
870-890	ν_s $(Mo\text{-}O^-)_{tet}$	41, 50-52
875-955	ν_s $(W\text{-}O^-)_{oct}$	41,43,49
885-950	ν_s $(Mo\text{-}O^-)_{oct}$	41, 50-52
935-985	ν_s (Mo=O),	41, 50
935-995	ν_s (W=O)	41,43,49
982	ν_s (PO_4), Q^0	41,45,46
1030	ν_s (P-O), Q^1 chain terminator	41,45,46
1065-1100	ν_s (PO_3), Q^1	41,45,46
1140-1165	ν_s (PO_2), Q^2	41,45,46
1200-1270	ν_{as} (PO_2), Q^2	41,45,46

Indeed, significant changes in Raman spectra are observed with the addition of WO_3 to the silver-zinc phosphate glass, Figure 2(a). A new strong band appears at 937 cm^{-1} together with a shoulder at 875 cm^{-1} related to the vibration of terminal bonds in WO_6 octahedra, W=O and $W\text{-}O^-$, respectively [43,49]. With increasing WO_3 content up to 60 mol% maximum of the dominant band shifts to higher wavenumbers and retains its intensity, whereas the shoulder intensity decreases and completely disappears from the spectrum of glass containing 60 mol% WO_3. The observed shift is related to the deformation of WO_6 octahedra. Vibrational bands of phosphate Q^2 units at 1143 and 690 cm^{-1} decrease in strength with increasing WO_3 content partly due to the decrease of their content and partly due to a high efficiency of Raman scattering of tungsten units. Glass structure with up to 30 mol% of WO_3 is dominated by

metaphosphate (Q^2) chains interlinked with WO_6 octahedra which can be referred as the first step of structural transformation of phosphate glass network [41,43]. The additional confirmation of cross-linkage between phosphate chains and tungsten units is observed by the presence of a band at about 380 cm^{-1} related to the W-O-P bonds. Further, in Raman spectra of compositions containing ≥ 30 mol% WO_3 two new bands appear at 866 and 764 cm^{-1}. These bands are associated with symmetric and asymmetric stretching mode of bridging oxygen atoms within W-O-W bond in clusters [43,49] and their intensity increases with increase in WO_3 content. Thus, at high WO_3 content, the second step of transformation can be identified in which WO_6 octahedra form three-dimensional tungsten clusters involved in W-O-W bonding.

The evolution of Raman spectra of the Ag-Mo glasses, presented in Fig. 3(a), seems to be very similar to the spectra of Ag-W glasses, Fig. 2(a), especially for glasses containing up to 30 mol% of MoO_3. Doublet of bands in the range of 800-1000 cm^{-1} with the strong band at 935 cm^{-1} and a shoulder at 886 cm^{-1} ascribed to the vibration of terminal bonds, Mo=O or $Mo\text{-}O^-$ in MoO_6 octahedra, are present in the glass structure [50-52]. However, the decrease in the strength of vibrational bands related to phosphate units is faster than at the analogous WO_3 glasses implying a higher degree of depolymerization.

A detailed analysis of Raman spectra of the Ag-Mo glasses containing ≥30 mol% MoO_3 content reveals different structural evolution, as shown in Fig. 3(a). Firstly, the decrease in the intensity of the shoulder at 886 cm^{-1} related to MoO_6 octahedra is accompanied by the increasingly stronger additional band at 872 cm^{-1} which appears in the spectra. This new band corresponds to the MoO_4 tetrahedra [51] and its growth suggests a gradual change in the coordination of molybdenum, from dominantly six (MoO_6 octahedra) to dominantly four (tetrahedral MoO_4 units) as the MoO_3 content increases. Therefore, depending on composition, the glass network of Ag-Mo glasses in this study consists of both

MoO_4 tetrahedra and MoO_6 octahedra, and is consistent with the literature result on similar glasses [41]. Also, it should be noted that results on Ag-Mo glasses are in contrast to the Ag-W glasses, where in the whole compositional range the dominant tungstate units are WO_6 octahedra, Fig. 2(a).

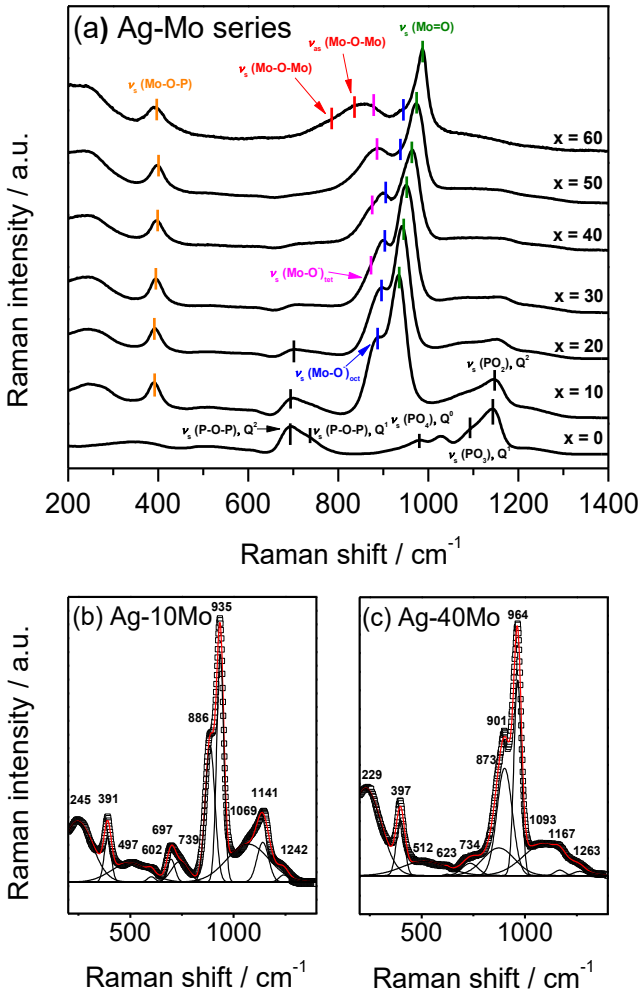

Fig. 3. (a) Raman spectra of $xMoO_3$-(30-0.5x)Ag_2O-(30-0.5x)ZnO-40P_2O_5 series of glass and deconvolution of the Raman spectra for (b) Ag-10Mo and (c) Ag-40Mo in the 200-1400 cm^{-1} region.

Secondly, the intensity of the vibrational band in the range 391-397 cm^{-1} attributed to the Mo-O-P bonds [51] steadily increases with increasing MoO_3 content indicating higher cross-linkage of phosphate and molybdenum units throughout the whole compositional range.

Moreover, unlike of Ag-W series where W-O-W bonds are present in glasses with WO_3 content as low as 30 mol%, the vibrational modes ascribed to the Mo-O-Mo bonds (839 and 781 cm^{-1}) appear only in the Raman spectrum of binary 40P-60Mo glass, Fig. 3(a). This clearly demonstrates the significantly weaker tendency of molybdenum units to form clusters in the glass structure.

Evidently different structural changes within Ag-W and Ag-Mo series explain trends in density in these series, as shown in Fig. 1(a-b). It seems that the growing fraction of MoO_4 tetrahedra interconnected with phosphate units and remaining MoO_6 octahedra does not allow close structural packing resulting in the decrease in glass density, whereas clustering of WO_6 octahedra produces highly dense glass structure which remains nearly constant over the entire compositional range. The former effect of more loosely bonded molybdenum and phosphate units is also reflected in the lower values of T_g and significantly higher values of thermal expansion coefficient, α, in glasses with higher MoO_3 content.

3.3. Electrical Transport

Conductivity isotherms of Ag-10W glass, as typical conductivity spectra for all glasses studied in this work, are shown in Fig. 4(a). Characteristically, each isotherm exhibits two features, a plateau at a low frequency that corresponds to the DC conductivity and dispersion at higher frequencies. The DC conductivity exhibits Arrhenius temperature dependence and hence has characteristic activation energy, see Fig. 4(b). The dispersive behavior is more visible at lower frequencies and temperatures, and shifts to higher frequencies at higher temperatures. In general, conductivity dispersion is characteristic for ionic as well as polaronic glasses [53] and, hence, it is not connected to the type of charge carriers. Instead, it is closely related to the structural disorder, one property which is common to all glasses.

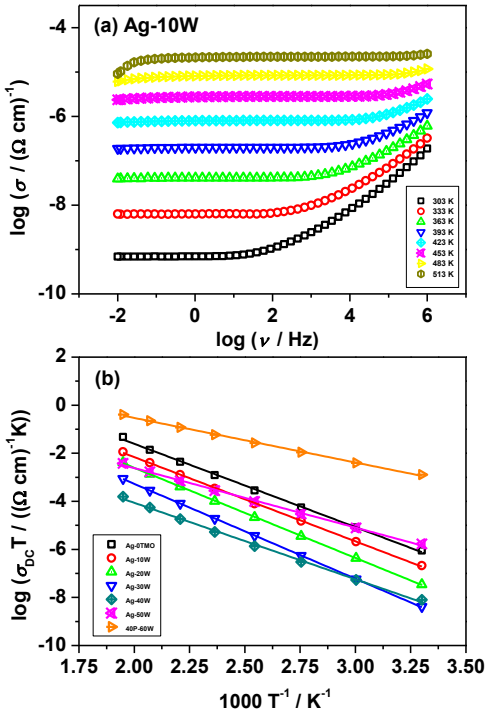

Fig. 4. (a) Conductivity spectra at different temperatures for Ag-10W glass and (b) Arrhenius plots of the temperature dependence of DC conductivity for Ag-W series of glasses.

In addition to the two observed spectral features, glasses containing a high amount of Ag_2O exhibit a slight decrease in conductivity at higher temperatures and in the low-frequency region as is visible in conductivity spectrum of Ag-10W glass at 513 K, as shown in Fig. 4(a). This behavior is associated with the electrode polarization effect due to the accumulation of mobile silver ions at the blocking metallic electrode. Naturally, with increasing WO_3 and decreasing Ag_2O content in the studied glasses the effect of electrode polarization decreases and finally completely disappears from the conductivity spectra of pure polaronic glasses, namely 40P-60W and 40P-60Mo.

3.3.1. DC conductivity and activation energy

Fig. 5(a-b) shows a compositional dependence of DC conductivity at various temperatures for Ag-W and Ag-Mo series of glasses. Starting TMO-free glass with 30 mol%

of Ag_2O exhibits high DC conductivity of 2.97×10^{-9} $(\Omega\ cm)^{-1}$ at 303 K, which decreases with gradual addition of TMOs and decrease in Ag_2O content.

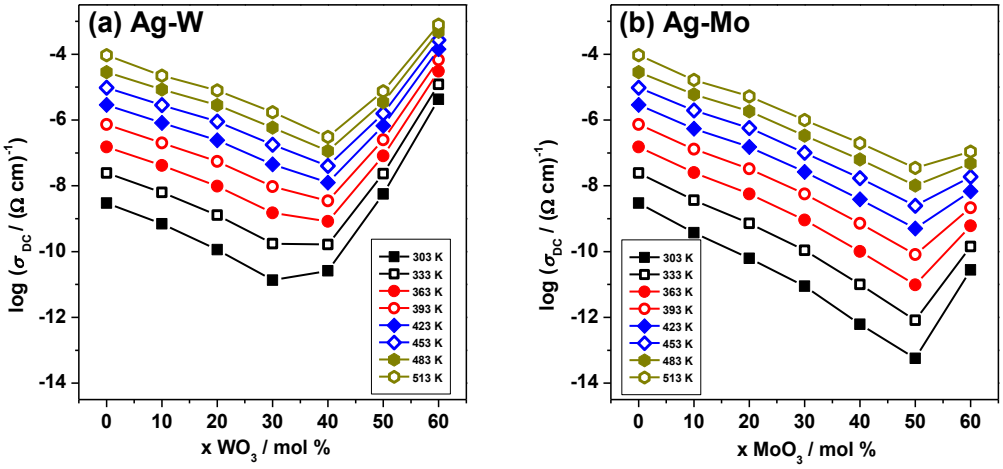

Fig. 5. DC conductivity trends at various temperatures for investigated (a) Ag-W and (b) Ag-Mo series of glasses.

However, the complete replacement of Ag_2O with TMO within these two series induces different changes in DC conductivity. For Ag-W glasses, Fig. 5(a), the DC conductivity passes through a minimum at approximately 30-40 mol% of WO_3 and sharply increases for several orders of magnitude with further increase in WO_3 content reaching the highest value for binary 40P-60W glass of 4.26×10^{-6} $(\Omega\ cm)^{-1}$ at 303 K. On the other hand, as Ag_2O becomes entirely replaced by MoO_3 the DC conductivity decreases linearly and a slight increase is observed only for binary 40P-60Mo glass which is completely free of Ag_2O.

The observed minimum in conductivity for Ag-W glasses suggests a changeover from predominantly ionic to predominantly polaronic conductivity. Below 30 mol% of WO_3, the dominant conduction mechanism is ionic and, hence, it is determined by the number density of highly mobile silver ions, whereas for the glasses with higher WO_3 content the DC conductivity increases due to an increased contribution of polaronic conduction which includes transfer of electrons between W^{5+} and W^{6+} ions. The exchange of the predominance of transport mechanisms is also reflected in the shift of the conductivity minimum to the

higher WO_3 content with increasing temperature, being 30 mol% at 303 K and 40 mol% at 513 K, as shown in Fig. 5(a). The observed effect is associated with a stronger influence of temperature on the mobility of Ag^+ ions than polarons, which in turn changes the relative contributions of the two conduction mechanisms to the total conductivity in this narrow compositional range. In contrast to tungsten glasses, the trend in DC conductivity for Ag-Mo glasses indicates that the electrical transport is dominated by the highly mobile silver ions without significant polaronic contribution through the electron transfer between Mo^{5+} and Mo^{6+} ions. Certainly, the binary 40P-60Mo glass with slightly higher conductivity is a purely polaronic conductor.

Considering the nature of polaronic transport and its contribution to the total conductivity in these glasses, it is important to discuss basic factors that determine it. Besides the type and total amount of TMO present in the glass, the polaronic conductivity strongly depends on the fraction of transition metal ions in different oxidation states. As can be seen from the Table 1, the fractions of W^{5+}/W_{tot} and Mo^{5+}/Mo_{tot} increases continuously up to 1.45% and 37.04%, respectively, with increasing TMO content up to 60 mol% of WO_3 and MoO_3, thus demonstrating an increase in polaronic number density as a general trend in both glass series.

While the increase of transition metal fractions with an increase of the total TMO amount agrees well with the takeover of polaronic transport over ionic one for glasses with ≥ 30 mol% of WO_3, it fails to explain the trend in DC conductivity of glasses containing MoO_3, as shown in Fig. 5. Besides that, due to a stronger reduction tendency of molybdenum in the melting process [54], fractions of Mo^{5+}/Mo_{tot} are drastically higher than that of W^{5+}/W_{tot} throughout the whole compositional range. Therefore, one would easily assume that the contribution of polaronic transport would be much higher in glasses containing MoO_3. However, the trends in DC conductivity, shown in Fig. 5, prove just the opposite. In

particular, the purely polaronic glass $60WO_3$-$40P_2O_5$ (mol%) has more than five orders of magnitude higher conductivity at 303 K than purely polaronic $60MoO_3$-$40P_2O_5$ (mol%) despite the fact that W^{5+}/W_{tot} is only 1.45%. This apparently counterintuitive result has its origin in different structural features of glasses containing WO_3 and MoO_3. While the addition of MoO_3 in silver zinc phosphate glasses induces a gradual change of MoO_6 octahedra to MoO_4 tetrahedra both being highly cross-linked with phosphate units throughout the whole compositional range, the introduction of WO_3 causes the clustering of WO_6 octahedra, as shown in Fig. 2 and 3. In fact, the clustering of tungsten units has been identified in glasses with WO_3 ≥30 mol% which is exactly the compositional region where the pronounced increase in DC conductivity occurs. Therefore, it can be concluded that the formation of W-O-W linkages in tungsten clusters drastically facilitates the polaronic transport giving rise to the high conductivity of glasses containing higher WO_3 content. In contrast, in glasses containing MoO_3 the polaronic transport is hindered by the interweaving of molybdenum and phosphate units and this hindrance cannot be compensated with drastically higher polaron number density. This undoubtedly points out that the most important role for polaronic transport in these glasses plays the structure and not the polaron number density determined from the overall TMO content and fraction of transition metal ions in different oxidation state.

The change in the mechanism of conduction within these two series is also reflected in the changes of the activation energy for DC conductivity, E_{DC}. The DC conductivity of all glasses exhibits Arrhenius temperature dependence [41,55,56], so the E_{DC} for each sample is determined from the slope of log $\sigma_{DC}T$ vs. 1000/T using the equation:

$$\sigma_{DC}T = \sigma_0^* \exp(-E_{DC}/k_B T) \qquad (1)$$

where k_B is the Boltzmann constant and T is the temperature (K). The activation energy, E_{DC}, for Ag-W and Ag-Mo glasses exhibit a steep decrease above 30 mol% and 50 mol% of WO_3 and MoO_3, respectively, Table 3 and Fig. S1.

It is expected that a decrease in DC conductivity is related to the increase in the activation energy and *vice versa*. As it can be seen in Table 3 and Fig. S1, the trends of these two variables within Ag-W and Ag-Mo series show expected behavior and reflect the changes in the prevalence of the ionic or polaronic transport mechanism.

Table 3. DC conductivity, σ_{DC}, activation energy, E_{DC}, and pre-exponential factor, σ_0^*, for all investigated glasses.

Glass	σ_{DC}[a] / $(\Omega\ cm)^{-1}$ ± 0.5%	E_{DC} / eV ± 0.5%	log σ_0^* / $(\Omega\ cm)^{-1}$ K ± 0.5%
WO_3-Ag_2O-ZnO-P_2O_5			
Ag-0TMO	2.97×10^{-9}	0.69	5.32
Ag-10W	6.95×10^{-10}	0.69	4.85
Ag-20W	1.16×10^{-10}	0.74	4.89
Ag-30W	1.35×10^{-11}	0.78	4.62
Ag-40W	2.61×10^{-11}	0.63	2.29
Ag-50W	5.62×10^{-9}	0.49	2.33
40P-60W	4.26×10^{-6}	0.37	3.18
MoO_3-Ag_2O-ZnO-P_2O_5			
Ag-0TMO	2.97×10^{-9}	0.69	5.32
Ag-10Mo	3.74×10^{-10}	0.72	4.91
Ag-20Mo	6.19×10^{-11}	0.76	4.83
Ag-30Mo	8.85×10^{-12}	0.77	4.28
Ag-40Mo	6.12×10^{-13}	0.84	4.26
Ag-50Mo	5.62×10^{-14}	0.89	3.95
40P-60Mo	2.75×10^{-11}	0.56	1.21

[a] values at 303 K

However, the DC conductivity of specific mixed ionic-electronic glass comprises both contributions and based on this value alone it is not possible to identify them. As a step forward, we attempt to gain more insight into the nature of mixed electrical transport in these glasses by analyzing the frequency dependence of complex impedance which allows the separation of different contributions on the frequency scale.

3.3.3. Complex impedance plots

The results of impedance spectroscopy measurements for selected glasses are presented in complex impedance plane, Fig. 6(a-d), as imaginary, *Z''*, against the real, *Z'*, part, while both quantities are frequency dependent.

The complex impedance plot of glasses with predominantly ionic conductivity, such as Ag-10W glass, consists of a single semicircle that emanates from bulk conduction and a low-frequency spur related to the electrode polarization, as shown in Fig. 6(a). On the opposite side of the compositional region, binary 40P-60W and 40P-60Mo glasses (Fig. 6(b)) exhibit single impedance semicircle without any signature of electrode polarization which is, taking composition into account, characteristic for purely polaronic conductors [34,57,58].

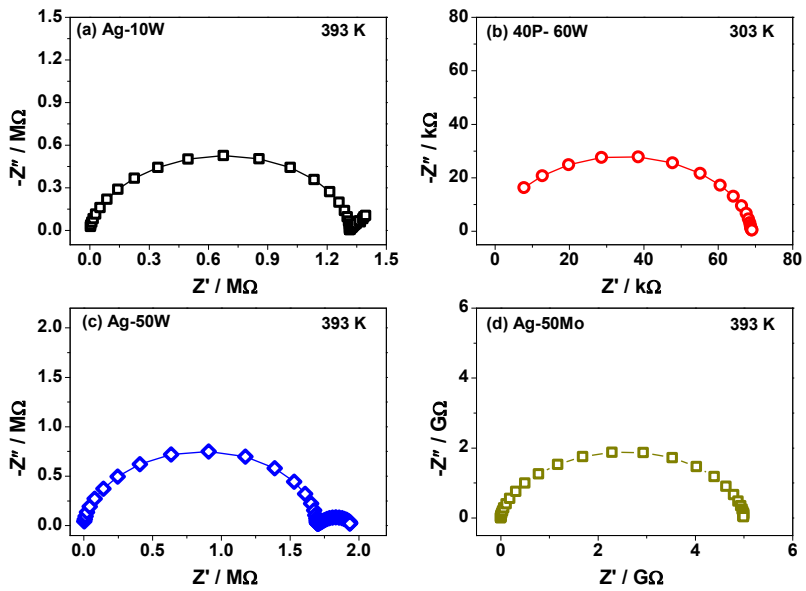

Fig. 6. Complex impedance plots for selected glasses (a) Ag-10W, typical ionic plot; (b) 40P-60W glass, typical polaronic plot and two cases of mixed composition ionic-TMO glasses (c) Ag-50W and (d) Ag-50Mo.

However, an interesting result is obtained for Ag-50W glass (Fig. 6(c)) where two distinct semicircles are present in the complex impedance plot. In literature, such a behavior is

reported for glass systems which exhibit coexistence of polaronic and ionic conduction [34,39,41,57-60]. Actually, it is found to be typical for mixed ionic-polaronic conduction when selectively blocking electrodes (e.g. blocking for one carrier and non-blocking for the other one) are used. In our case, gold electrodes, which are blocking for ions and non-blocking for polarons, were applied for electrical measurements. Therefore, the high-frequency semicircle observed for Ag-50W glass (Fig. 6(c)) can be assigned to the dielectric relaxation of bulk, whereas the additional semicircle at lower frequencies refers to a chemical relaxation due to unblocked polaronic diffusion [57,58]. In particular, close inspection of the low-frequency semicircle (Fig. 6(c)) reveals a typical Warburg-type response with an inclination of the line close to 45° suggesting a significant polaronic contribution. Here, it should be noted that the low-frequency semicircle can be erroneously attributed to the contact effects due to the roughness of the glass surface or partial crystallization of the glass. However, since XRD analysis confirmed the amorphous nature of this glass and repeated polishing of the glass surface had no effect on the complex impedance plots, it should be concluded that the two separated semicircles originate from the existence of two different transport mechanism, ionic and polaronic in the Ag-50W glass.

It is interesting to note that the two semi-circles in the complex impedance plane are observed only for Ag-50W glass, as shown in Fig. 6. The DC conductivity of this glass lies on the polaronic side above the conductivity minimum where the takeover of polaronic over ionic conduction is expected to start, see Fig. 5(a). Therefore, for this particular mixed conductor, the ratio of both contributions, ionic and polaronic allows their identification in a complex impedance plane [57,58]. This conclusion is also supported by the fact that all glasses from Ag-Mo series show only one impedance semicircle, Fig. 6(d), since in this glass series a steady linear decrease of DC conductivity is observed in the entire mixed Ag-Mo compositional range, with the addition of MoO_3 from 10 to 50 mol%. Such behavior indicates

that the polaronic conduction is hindered and its contribution is not large enough to increase the total electrical conductivity.

Up to this point, we showed how the type of TMO (WO_3; MoO_3) can influence the overall electrical transport in studied mixed ion-polaron zinc phosphate glasses. In the next step, we attempt to clarify the role of cation-type (Ag^+, Na^+, and Li^+) in the ionic transport in these mixed conducting glasses.

3.3.3. Ag^+ *vs* Na^+ and Li^+ transport in TMO - zinc phosphate glasses

Besides surprisingly high polaronic conductivity related to the introduction of WO_3, glasses with higher Ag_2O content are characterized by high ionic conductivity. In our recent work [41] we have studied the mixed ion-polaron conduction in analogous WO_3/MoO_3 zinc phosphate glasses containing Li_2O/Na_2O (instead of Ag_2O) and observed significantly lower ionic conductivity of Li^+ and Na^+ ions, as shown in Fig. 7.

From Fig. 7 it can be seen that the DC conductivity of purely ionic Ag-0TMO glass, at 303 K, is four orders of magnitude higher than Li-0TMO and Na-0TMO glasses where DC conductivities are as low as 1.94×10^{-13} and 7.87×10^{-13} $(\Omega\ cm)^{-1}$, respectively. Further, comparing all glass series containing WO_3, the DC conductivity of glasses with Li_2O exhibits a clear minimum at 20 mol% Li_2O and 20 mol% WO_3 indicating the cross-over point between predominance areas of ionic and polaronic conductivity similarly as in glasses containing Ag_2O. The shift of the minimum towards the lower Ag_2O and higher WO_3 content is related to the significantly higher mobility of silver ions which compensates the decrease in their number density keeping the ionic conductivity contribution to the total conductivity high. Indeed, at low WO_3 content, where the ionic conductivity dominates, the DC conductivity decreases in the following order $Ag_2O>Na_2O>Li_2O$, as shown in Fig. 7(a). Since the glass compositions in all three series are analogous and, thus, the number density of ionic species is

almost equal (taking into account slight variations in density) the plausible explanation for the differences in ionic conductivity is their different mobility.

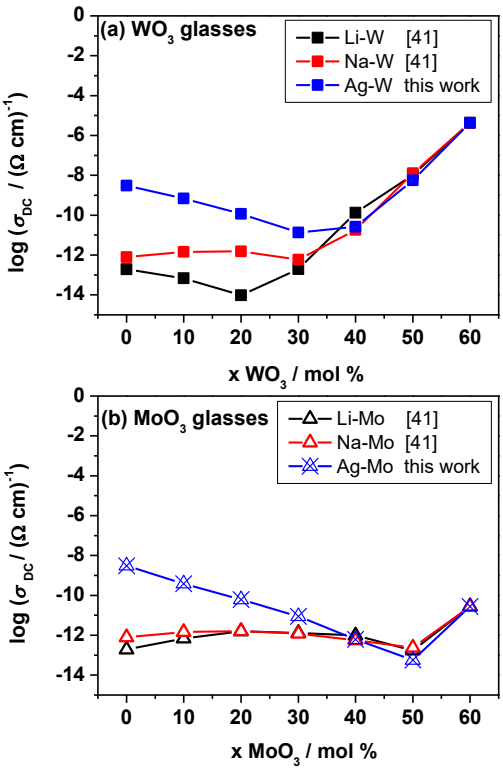

Fig. 7. Compositional dependence and mutual comparison of DC conductivity, σ_{DC}, at 303 K for (a) WO_3 glass series (full squares) and (b) MoO_3 glass series (open triangles) with Ag_2O from this work and Li_2O and Na_2O from Ref [41].

In our case, the mobility of ionic species follows the trend in their ionic radii, being 90, 116 and 129 pm for Li^+, Na^+, and Ag^+, and increases in the opposite order than their polarization power. This observation suggests that the critical factor which determines ionic mobility in these glasses is the interaction of mobile cations with the glass network, and not their size. From the Raman spectra of analogous WO_3 glasses containing Li_2O, Na_2O, and Ag_2O (Fig. 2. in this work and [41]), almost identical structural features can be identified which imply that similar local surrounding is provided for either Ag^+, Na^+ or Li^+ ions. The only difference is slightly earlier formation of tungsten clusters, 20 mol% Na_2O and Li_2O in comparison to 30 mol% of Ag_2O, which corresponds well with the DC minimum and the takeover of polaronic

conductivity in the glasses with higher WO_3 content, as shown in Fig. 7(a). In this context, it is expected that Li^+ ions form very tight linkages with the terminal non-bridging oxygens in depolymerized phosphate network which results in their weak mobility and hence the lowest conductivity. Further, despite their bigger size, Na^+ ions are slightly more mobile because of their lower ability to polarize the network, and finally, loosely bonded Ag^+ ions are highly mobile giving rise to the highest ionic conductivity.

Further, it is interesting to consider the influence of MoO_3 on the transport of Ag^+, Na^+, and Li^+ ions, comparing Fig. 7(a) and (b). While the glasses containing higher amounts of Ag_2O and Na_2O, between 15 and 30 mol%, exhibit almost identical DC conductivity regardless of the type of the incorporated tungsten or molybdenum units, obvious difference in DC conductivity is observed in the case of glasses with Li_2O content. In the compositional range up to 30 mol% of WO_3/MoO_3, where the ionic transport prevails, the DC conductivity of Li-W glasses changes in a non-monotonic fashion exhibiting minimum, whereas for Li-Mo glasses it remains nearly constant, as shown in Fig. 7(a) and (b). Interestingly, the Raman spectra of the corresponding Li-W and Li-Mo glasses show only a slight structural difference evident in the fact that incorporation of MoO_6 octahedra depolymerizes phosphate network more strongly than WO_3 octahedra [41]. Although this structural feature is also observed, in somewhat smaller extent, in glasses containing Ag_2O and Na_2O it seems that it affects only the transport of Li^+ ions in more depolymerized phosphate network containing MoO_6 octahedra keeping the conductivity constant. On the other hand, Na^+ and Ag^+ ions are not affected by such slight structural deviations since they both tend to form weaker bonds and, hence, are less sensitive to the changes in the local structural environment.

Still, a considerably higher mobility of Ag^+ in comparison to other alkali ions in these glasses is fascinating. An exceptionally high Ag^+ mobility is found in various

silver phosphate glasses doped with silver halide [61,62] and silver chalcogenide [63] where high conductivity is achieved by the increase of the conduction pathway volume due to expanding of the glass network [64-66]. Such an increase in the distance between the phosphate units results in a weakening of the Coulomb interactions between Ag^+ and anion units in glass network leading to facilitated ionic transport. Although there is an obvious difference in the structure of glasses from this study and those doped with silver halide, both families of glasses bring forward the unique character of Ag^+ ions to interact loosely with the local neighborhood in glass network.

Going back to the complexity of mixed ion-polaron conduction and conditions for the dominance of each contribution, we have analyzed the electrical parameters of all six $Li_2O/Na_2O/Ag_2O–WO_3/MoO_3–ZnO–bP_2O_5$ above discussed glass series using Meyer-Neldel formalism [67]. The Meyer-Neldel rule is found to be valid for thermally activated processes in a wide range of materials, including ionic and mixed ionic-electronic glasses [68-74] as well as electronic amorphous or disordered semiconductors [75]. It states that the DC conductivity pre-exponential factor (σ_0*) correlates the activation energy for DC conductivity (E_{DC}) according to the following relation:

$$\log \sigma_0^* = aE_{\mathrm{DC}} + \mathrm{b} \qquad (2)$$

where a and b are constants. Here it is important to note that *a* is supposed to be positive so that Eq. (2) indicates that logσ_0* increases with increasing E_{DC}. However, in some cases [70-75], *a* is found to be negative and such a behavior is called anti-Meyer-Neldel rule. Although Meyer-Neldel relation suffers from the severe drawback of being an empirical model with the parameters that have no clear physical meaning [76], its results are consistent with

experimental data and the change of sign of parameter *a* points toward the change in the conduction mechanism [73,74].

Without any doubt, the correlation between σ_0* and E_{DC} for all glasses containing WO_3 (Fig. 8(a)) exhibits two distinct domains with different signs of slope (parameter *a*). The Domain I contains glasses with high concentration of mobile ions (≥15 mol% Ag_2O, ≥15 mol% Na_2O and ≥20 mol% Li_2O) and shows a positive correlation, whereas the rest of the glasses fall into the Domain II exhibiting a negative slope.

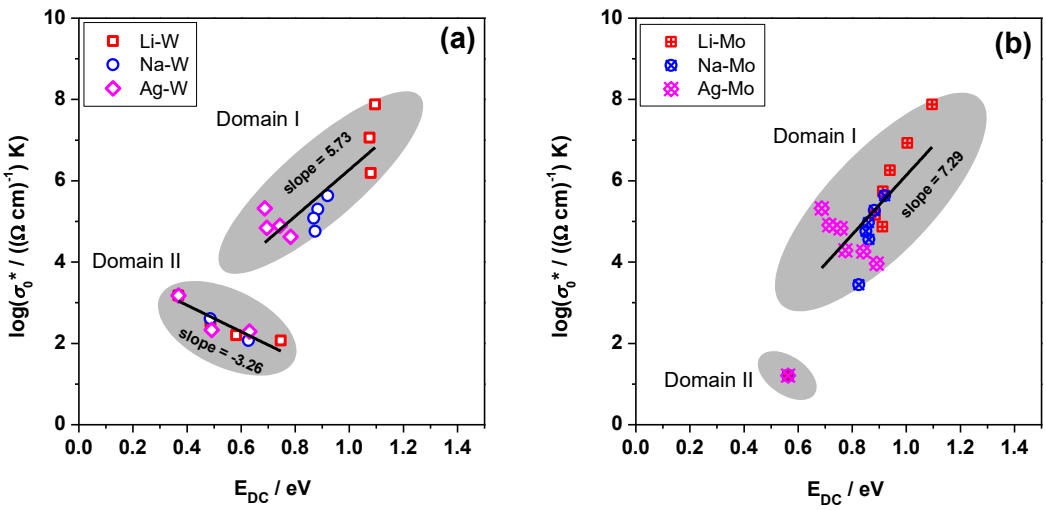

Fig. 8. Compositional dependence of pre-exponential factor, σ_0*, plotted as a function of activation energy, E_{DC} for series of glasses containing: (a) WO_3 and (b) MoO_3. Data for Li_2O and Na_2O containing glasses are from Ref [41].

Obviously, the positive and the negative correlations are related to the nature of electrical transport mechanism and show a predominance of ionic (Domain I) and polaronic (Domain II) conduction mechanism. Relating these results with the trends in conductivity it can be observed that for all three series, glasses grouped in the Domain II correspond to the polaronic region which spans from one glass above the DC conductivity minimum up to the purely polaronic 40P-60W glass, as seen in Fig. 7(a).

On the other hand, all glasses containing MoO_3 show a positive correlation between σ_0* and E_{DC} (Fig. 8(b)) except of purely polaronic 40P-60Mo glass which clearly departs from the line. This again supports our previous conclusion that the contribution of polaronic transport introduced by MoO_3 is considerably low. Given all these considerations, it can be inferred that the analysis of the correlation between pre-exponential factor and activation energy as proposed by Meyer-Neldel formalism allows for a clear identification of the prevalence of ionic or polaronic conduction mechanism in the studied glasses.

Finally, this study reveals that Ag_2O-WO_3-ZnO-P_2O_5 glass system exhibits significant and well-distinguished contributions of ionic or polaronic conductivity depending on composition and thus shows a promise as an electrically tuneable cathode material. However, for development of these mixed ion-polaron conducting glasses it would be beneficial to perform the multivariate study, in particular a design of experiments (DoE) [77,78,79,80], probing the influence of the glass composition (type and amount of TMO and mobile cation, the fraction of TM ions in different oxidation states), experimental conditions (temperature and frequency) on physical parameters such as DC, AC conductivity and dielectric permittivity. Such thorough chemometric approach, which is planned for future work, will help identify the most relevant variables and their mutual interactions which is essential for optimization of these materials.

4. Conclusion

The influence of gradual exchange of Ag_2O by transition metal oxide content, WO_3 and MoO_3, on the nature of electrical transport in two series of glasses with the compositions xTMO-(30-0.5x)Ag_2O-(30-0.5x)ZnO-40P_2O_5 (TMO=MoO_3/WO_3, $0 \leq x \leq 60$ mol%) is studied by impedance spectroscopy over a wide frequency and temperature range. Observed structural

changes as a result of variation of content and type of TMO showed once again the beauty of glass structure complexity which plays a key role in the nature of electrical transport is these mixed ionic-polaronic glasses.

The obtained results reveal a strong compositional dependence and different behavior of DC conductivity at temperatures between 303 and 513 K for either tungsten or molybdenum glasses containing Ag_2O. For WO_3 series, the transition from ionic to polaronic conductivity is observed with a clear minimum at 30-40 mol% of WO_3 content in DC conductivity where the beginning of clustering of tungsten units is identified. Formation of W-O-W linkages in glasses with high WO_3 content facilitates polaronic transport reaching the highest value in conductivity for pure binary tungsten glass. On the other hand, the addition of MoO_3 in silver zinc phosphate glasses induces a gradual change of MoO_6 octahedra to MoO_4 tetrahedra both being highly cross-linked with phosphate units via P-O-Mo bonds throughout the whole compositional range, without clustering of MoO_6 octahedra at high MoO_3 content. DC conductivity for MoO_3 glasses decreases in the whole mixed Ag-Mo compositional range, in contrast to WO_3-series. Thus indicating that the nature of electrical transport is dominated by ionic component due to highly mobile Ag^+ without a significant contribution of polaronic mechanism, although the concentration of Ag^+ ions decreases and simultaneously MoO_3 content increases. Change in the predominant electrical transport also reflects on the shape of the complex impedance plot. Two semi-circles are observed only for Ag-50W glass, which lies above the conductivity minimum where the takeover of polaronic over ionic conduction is expected. The ratio of ionic and polaronic contribution for this mixed conductor allows their identification in a complex impedance plane. Furthermore, despite a significantly lower fraction of W^{5+}/W_{tot}, a binary 40P-60W glass exhibits more than five orders of magnitude higher conductivity at 303 K than pure polaronic 40P-60Mo glass (4.26×10^{-6} $(\Omega\ cm)^{-1}$ *vs.* 2.76×10^{-11} $(\Omega\ cm)^{-1}$). Once again, high DC conductivity value for $40P_2O_5$-$60WO_3$ glass is

related to the formation of tungsten clusters which form continuous W^{5+}-O-W^{6+}-O-W^{5+}-O-W^{6+} bridges and drastically facilitate the possibility of polaronic transport. In contrast, in glasses containing MoO_3 polaronic transport is hindered and cannot be compensated with drastically higher polaron number density.

Finally, we attempt to clarify the role of cation-type such as Ag^+, Na^+ and Li^+ ions on the electrical transport in these mixed ion-polaron glasses. Strong correlations are found between pre-exponential factor and activation energy of DC conductivity, as proposed by Meyer-Neldel formalism, which allowed us to distinctly identify two domains with the prevalence of ionic or polaronic conduction mechanism in studied glasses. Moreover, detail analysis of cation-type role clearly showed that the degree of linkage looseness of the cations to the network units, in studied glasses, follows this order $Ag^+ > Na^+ > Li^+$. This leads to the conclusion that the weakening of Coulombic interactions between Ag^+ and anionic units results in the easier creation of conduction pathways for highly mobile Ag^+ ions in the glass network. As a result, facilitates fast ionic transport thus giving rise to the highest ionic conductivity for Ag-rich glasses throughout the measured temperature range.

5. Acknowledgements

This work was supported by the Croatian Science Foundation; project IP-09-2014-5863. D.P. would like to acknowledge the partial support of Croatian Science Foundation; project UIP-2014-09-8276. The Czech authors are grateful for the financial support from the project No. 18-01976S of the Grant Agency of the Czech Republic.

.

References

[1] C. Cao, Z. B. Li, X. L. Wang, X. B. Zhao, W. Q. Han, Recent advances in inorganic solid electrolytes for lithium batteries, Frontiers in Energy Research 2 (2014), 1-10, doi.org/10.3389/fenrg.2014.00025.

[2] N. Baskaran, G. Govindaraj, A. Narayanaswamy, Solid-state batteries using silver-based glassy materials, J. Power Sources 55 (1995) 153–157, doi.org/10.1016/0378-7753(95)02183-H.

[3] A. Chandra, A. Bhatt, A. Chandra, Ion conduction in superionic glassy electrolytes: an overview, J. Mater. Sci. Technol. 29 (2013) 193–208, doi.org/10.1016/j.jmst.2013.01.005.

[4] S. Afyon, F. Krumeich, C. Mensing, A. Borgschulte, R. Nesper, New high capacity cathode materials for rechargeable Li-ion batteries: vanadate-borate glasses, Scientific Reports 4 (2014) 7113, doi.org/10.1038/srep07113.

[5] S. Bhattacharya, D. Dutta, A. Ghosh, Dynamics of Ag^+ ions in Ag_2S-doped superionic $AgPO_3$ glasses, Phys. Rev. B 73 (2006), doi.org/10.1103/PhysRevB.73.104201.

[6] J. Kincs, S. W. Martin, Non-Arrhenius conductivity in glasses: mobility and conductivity saturation effects, Phys. Rev. Lett. 76 (1996) 70–73, doi.org/10.1103/PhysRevLett.76.70.

[7] T. Minami, K. Imazawa, M. Tanaka, Formation region and characterization of superionic conductivity glasses in the systems AgI-Ag2O-MxO7, J. Non-Cryst. Solids 42 (1980) 469–476, doi.org/10.1016/0022-3093(80)90045-9.

[8] C. Rousselot, J. P. Malugani, R. Mercier, M. Tachez, P. Chieux, A. J. Pappin, M. D. Ingram, The origins of neutron scattering prepeaks and conductivity enhancement in AgI containing glasses, Solid State Ionics 78 (1995) 211–221, doi.org/10.1016/0167-2738(95)00103-D.

[9] J. Ren, H. Eckert, Anion Distribution in Superionic Ag_3PO_4–AgI Glasses Revealed by Dipolar Solid-State NMR, J. Phys. Chem. C 117 (2013) 24746−24751, doi.org/10.1021/jp409307c.

[10] S. Bhattacharya, A. Ghosh, Conductivity spectra in fast ion conducting glasses: Mobile ions contributing to transport process, Phys. Rev. B 70 (2004) 172203, doi.org/10.1103/PhysRevB.70.172203.

[11] P. Boolchand, W. J. Bresser, Mobile silver ions and glass formation in solid electrolytes, Nature 410 (2001) 1070–1073, doi.org/10.1038/35074049.

[12] S. S. Das, C. P. Gupta, V. Srivastava, Ion transport studies in zinc/cadmium halide doped silver phosphate glasses, Ionics 11 (2005) 423–430, doi.org/10.1007/BF02430260.

[13] D. Rani, Solid State Batteries Based on Amorphous solids, in: Handbook of Solid State Batteries & Capacitors, ed. M. Z. A. Munshi, World Scientific Publishing, Singapore, Singapore, 1995.

[14] J. M. Reau, Liu Jun, B. Tanguy, J.J. Videau, J. Portier, P. Magenmuller, Influence of the S^{2-} = $2l^{-}$ substitution on the ionic conduction properties of the Ag^{+} glasses inside the $AgPO_3$-Ag_2S-AgI system, J. Solid State Chemistry, 1990, 85, 228–234, doi.org/10.1016/S0022-4596(05)80079-9.

[15] D. I. Novita, P. Boolchand, M. Malki, M. Micoulaut, Fast-Ion Conduction and Flexibility of Glassy Networks, Phys. Rev. Lett. 98 (2007) 195501, doi.org/10.1103/PhysRevLett.98.195501.

[16] I. Konidakis, C.P.E. Varsamis, E.I. Kamitsos, Effect of synthesis method on the structure and properties of $AgPO_3$-based glasses, J. Non-Cryst. Solids 357 (2011) 2684–2689, doi.org/10.1016/j.jnoncrysol.2011.03.013.

[17] S. M. Hsu, S.W. Yung, R.K. Brow, W.L. Hsu, C.C. Lu, F.B. Wu, S.H. Ching, Mater. Chem. Phys 123 (2010) 172–176, doi.org/10.1016/j.matchemphys.2010.03.078.

[18] K. Sklepić, M. Vorokhta, P. Mošner, L. Koudelka, A. Moguš-Milanković, Electrical Mobility of Silver Ion in Ag_2O–B_2O_3–P_2O_5–TeO_2 Glasses, J. Phys. Chem. B 118 (2014) 12050-12058, doi.org/10.1021/jp5073796.

[19] R. A. Montani, M. A. Frechero, The conductive behaviour of silver vanadium–molybdenum tellurite glasses, Solid State Ionics 158 (2003) 327-332., doi.org/10.1016/S0167-2738(02)00902-5.

[20] P. E. di Prátula, S. Terny, E. C. Cardillo, M. A. Frechero, The influence of transition metal oxides type M^{+}/M^{++} on the vanadium–tellurite glasses electrical behavior, Solid State Sciences 49 (2015) 83–89, doi.org/10.1016/j.solidstatesciences.2015.10.001.

[21] C. Dyre, P. Maass, B. Roling, D. L. Sidebottom, Fundamental questions relating to ion conduction in disordered solids, *Rep. Prog. Phys.* 72 (2009) 046501, doi.org/10.1088/0034-4885/72/4/046501.

[22] S. W. Martin, Ionic Conduction in Phosphate Glasses, J. Am. Ceram. Soc. 74 (1991) 1767–1784, doi.org/10.1111/j.1151-2916.1991.tb07788.x.

[23] I. G. Austin, Polaron conduction in disordered 3d oxides, J. Non-Cryst. Solids 2 (1970) 474–483, doi.org/10.1016/0022-3093(70)90161-4.

[24] N.F. Mott, Conduction in glasses containing transition metal ions, J. Non-Cryst. Solids 1 (1968) 1–17, doi.org/10.1016/0022-3093(68)90002-1.

[25] I. G. Austin, N.F. Mott, Polarons in crystalline and non-crystalline materials, Adv. Phy. 18 (1969) 41–102, doi.org/10.1080/00018736900101267.

[26] J. B. Goodenough, Y. Kim, Challenges for Rechargeable Li Batteries, Chem. Mater. 22 (2010) 587–603, doi.org/10.1021/cm901452z.

[27] M. Park, X. Zhang, M. Chung, G. B. Less, A. M. Sastry, A Review of Conduction Phenomena in Li-Ion Batteries, J. Power Sources 195 (2010) 7904–7929, doi.org/10.1016/j.jpowsour.2010.06.060.

[28] N. Nitta, F. Wu, J. T. Lee, G. Yushin, Li-ion battery materials: present and future, Materials today 18 (2015) 252–264, doi.org/10.1016/j.mattod.2014.10.040.

[29] H. Huang, S.-C. Yin, L. F. Nazar, Approaching Theoretical Capacity of $LiFePO_4$ at Room Temperature at High Rates, Electrochem. Solid-State Lett. 4 (2001) A170–A172, doi.org/10.1149/1.1396695.

[30] C. Wang, J. Hong, Ionic/Electronic Conducting Characteristics of LiFePO4 Cathode Materials, Electrochem. Solid-State Lett. 10 (2007) A65–A69, doi.org/10.1149/1.2409768.

[31] J. Ma, C. Wang, S. Wroblewski, Kinetic characteristics of mixed conductive electrodes for lithium ion batteries, J. Power Sources 164 (2007) 849–856, doi.org/10.1016/j.jpowsour.2006.11.024.

[32] I. Riess, The CRC Handbook of Solid State Electrochemistry, ed. P. J. Gellings, H. J. M. Bouwmeester, CRC Press, Boca Raton, 1997.

[33] C. Bazan, J. A. Duffy, M. D. Ingram, M. R. Mallace, Conductivity anomalies in tungstate-phosphate glasses: evidence for an ion-polaron interaction?, Solid State Ionics 86-88 (1996) 497–501, doi.org/10.1016/0167-2738(96)82669-5.

[34] J. E. Garbarczyk, P. Machowski, M. Wasiucionek, L. Tykarski, R. Bacewicz, A. Aleksiejuk, Studies of silver–vanadate–phosphate glasses by Raman, EPR and impedance spectroscopy methods, Solid State Ionics 136-137 (2000) 1077–1083, doi.org/10.1016/S0167-2738(00)00504-X.

[35] J. E. Garbarczyk, P. Machowski, M. Wasiucionek, W. Jakubowski, Electrical properties of AgI–Ag_2O–V_2O_5–P_2O_5 glasses, Solid State Ionics 157 (2003) 269-273, doi.org/10.1016/S0167-2738(02)00220-5.

[36] F. Salman, R. Khalil, H. Hazaa, Impedance measurements of some silver ferro-phosphate glasses, Adv. Mater. Lett. 7 (2016) 593–598, doi.org/10.5185/amlett.2016.6175.

[37] P. Jozwiak, J. E. Garbarczyk, Mixed electronic–ionic conductivity in the glasses of the Li_2O–V_2O_5–P_2O_5 system, Solid State Ionics 176 (2005) 2163–2166, doi.org/10.1016/j.ssi.2004.06.028.

[38] L. Bih, L. Abbas, A. Nadiri, H. Khemakhem, B. Elouadi, Investigations of molybdenum redox phenomenon in Li_2O–MoO_3–P_2O_5 phosphate glasses, J. Mol. Struct. 872 (2008) 1–9, doi.org/10.1016/j.molstruc.2007.02.005.

[39] B. Sujatha, R. Viswanatha, H. Nagabushana, C. N. Reddy, Electronic and ionic conductivity studies on microwave synthesized glasses containing transition metal ions, J. Mater. Res. Technol. 6 (2017) 7–12, doi.org/10.1016/j.jmrt.2016.03.002.

[40] R. A. Montani, M. A. Frechero, Mixed ion-polaron transport in lithium vanadium–molybdenum tellurite glasses, Solid State Sciences 177 (2006) 2911–2915, doi.org/10.1016/j.ssi.2006.08.015.

[41] J. Nikolić, L. Pavić, A. Šantić, P. Mošner, L. Koudelka, D. Pajić, A. Moguš-Milanković, Novel insights into electrical transport mechanism in ionic-polaronic glasses, J. Am Ceram. Soc., DOI:10.1111/jace.15271.

[42] N. H. Ray, Composition—property relationships in inorganic oxide glasses, J. Non-Cryst. Solids 15 (1974) 423−434, doi.org/10.1016/0022-3093(74)90148-3.

[43] C. C. de Araujo, W. Strojek, L. Zhang, H. Eckert, G. Poirier, S. J. L. Riberio, Y. Messaddeq, Structural studies of $NaPO_3$–WO_3 glasses by solid state NMR and Raman spectroscopy, J. Mater. Chem. 16 (2006) 3277–3284, doi.org/10.1039/B605971F.

[44] A. M. Nassar, M. M. El Oker, Sh. N. Radwan, E. Nabhan, Effect of MO (CuO, ZnO, and CdO) on the compaction of sodium meta phosphate sealing glass, Curr. Sci. Int. 2 (2013) 1-7, http://www.curresweb.com/csi/csi/2013/1-7.pdf

[45] R. K. Brow, Review: the structure of simple phosphate glasses, J. Non-Cryst. Solids 263-264 (2000) 1–28, doi.org/10.1016/S0022-3093(99)00620-1.

[46] R. K. Brow, D. R. Tallant, S. T. Myers, C. C. Phifer, The short-range structure of zinc polyphosphate glass, J. Non Cryst. Solids 191 (1995) 45–55, doi.org/10.1016/0022-3093(95)00289-8.

[47] A. Moguš-Milanković, A. Gajović, A. Šantić, D. E. Day, Structure of sodium phosphate glasses containing Al_2O_3 and/or Fe_2O_3. Part I, J. Non-Cryst. Solids 289 (2001) 204–213, doi.org/10.1016/S0022-3093(01)00701-3.

[48] A. Moguš-Milanković, L. Pavić, S. T. Reis. D. E. Day, M. Ivanda, Structural and electrical properties of Li_2O–ZnO–P_2O_5 glasses, J. Non-Cryst. Solids 356 (2010) 715–719, doi.org/10.1016/j.jnoncrysol.2009.04.077.

[49] L. Koudelka, J. Šubčik, P. Mošner, I. Gregora, L. Montagne, L. Delevoye, Structure and properties of lead borophosphate glasses doped with molybdenum oxide, Phys. Chem. Glasses: Eur. J. Sci. Technol. B 53 (2012) 79–85, http://www.ingentaconnect.com/content/sgt/ejgst/2012/00000053/00000006/art00002.

[50] S. H. Santagnelli, C. C. de Araujo, W. Strojek, H. Eckert, G. Poirier, S. J. L. Riberio, Y. Messaddeq, Structural Studies of $NaPO_3$–MoO_3 Glasses by Solid-State Nuclear Magnetic Resonance and Raman Spectroscopy, J. Phys. Chem. B 111 (2007) 10109–10117, doi.org/10.1021/jp072883n.

[51] J. Šubčík, L. Koudelka, P. Mošner, L. Montagne, G. Tricot, L. Delevoye, I. Gregora, Glass-forming ability and structure of ZnO–MoO_3–P_2O_5 glasses, J. Non-Cryst. Solids 356 (2010) 2509–2516, doi.org/10.1016/j.jnoncrysol.2010.02.013.

[52] L. Koudelka, I. Rosslerova, J. Holubova, P. Mošner, L. Montagne, B. Revel, Structural study of PbO–MoO_3–P_2O_5 glasses by Raman and NMR spectroscopy, J. Non-Cryst. Solids 357 (2011) 2816–2821, doi.org/10.1016/j.jnoncrysol.2011.03.006.

[53] A. Šantić, R. D. Banhatti, L. Pavić, H. Ertap, M. Yüksek, M. Karabulut, A. Moguš-Milanković, Polaronic transport in iron phosphate glasses containing HfO_2 and CeO_2, Phys. Chem. Chem. Phys. 19 (2017) 3999–4009, doi.org/10.1039/C6CP04226K.

[54] G. Poirier, F. S. Ottoboni, F. C. Cassanjes, A. Remonte, Y. Messadeq, S. J. L. Ribeiro, Redox Behavior of Molybdenum and Tungsten in Phosphate Glasses, J. Phys. Chem. B 112 (2008) 4481–4487, doi.org/10.1021/jp711709r.

[55] A. Moguš-Milanković, L. Pavić, H. Ertap, M. Karabulut, Polaronic Mobility in Boron Doped Iron Phosphate Glasses: Influence of Structural Disorder on Summerfield Scaling, J. Am. Ceram. Soc. 95 (2012) 2007–2014, doi.org/ 10.1111/j.1551-2916.2012.05149.x.

[56] A. Šantić, A. Moguš-Milanković, Charge Carrier Dynamics in Materials with Disordered Structures: A Case Study of Iron Phosphate Glasses, Croatica Chemica Acta 85 (2012) 245-254, doi.org/10.5562/cca1989.

[57] J. Jamnik, J. Maier, Treatment of the Impedance of Mixed Conductors Equivalent Circuit Model and Explicit Approximate Solutions, J. Electrochem. Soc. 146 (1999) 4183–4188, doi.org/10.1149/1.1392611.

[58] J. Jamnik, J. Maier, S. Pejovnik, A powerful electrical network model for the impedance of mixed conductors, Electrochim. Acta, 44 (1999) 4139–4145, doi.org/10.1016/S0013-4686(99)00128-0.

[59] J. R. Macdonald, Theory of space-charge polarization and electrode-discharge effects, J. Chem. Phys. 58 (1973) 4982–5001, doi.org/10.1063/1.1679086.

[60] A. E. Javier, S. N. Patel, D. T. Hallinan Jr., V. Srinivasan, N. P. Balsara, Simultaneous Electronic and Ionic Conduction in a Block Copolymer: Application in Lithium Battery Electrodes, Angew. Chem. Int. Ed. 50 (2011) 9848–9851, doi.org/10.1002/anie.201102953.

[61] M. Cutroni, A. Mandanici, P. Mustarelli, C. Tomasi, Conductivity dynamical response in $(AgI)x(AgPO_3)1-x$ glasses, Solid State Ionics, 154-155 (2002) 713–717, doi.org/10.1016/S0167-2738(02)00432-0.

[62] L. Badr, Low Temperature Conductivity and Ion Dynamics in Silver Iodide-Silver Metaphosphate Glasses, Phys. Chem. Chem. Phys. 19 (2017) 21527–21531, doi.org/10.1039/c7cp03695g.

[63] M. Cutroni, A. Mandanici, A. Piccolo, C. Fanggao, G. A. Saunders, P. Mustarelli, Frequency and temperature dependence of a.c. conductivity of vitreous silver phosphate electrolytes, Solid State Ionics 90 (1996) 167–172, doi.org/10.1016/S0167-2738(96)00392-X.

[64] D. L. Sidebottom, Influence of cation constriction on the ac conductivity dispersion in metaphosphate glasses, Phys. Rev. B: Condens. Matter Mater. Phys. 61 (2000) 14507–14516, doi.org/10.1103/PhysRevB.61.14507.

[65] J. D. Wicks, L. Borjesson, G. Bushnell-Wye, W. S. Howells, R. L. McGreevy, Structure and Ionic Conduction in (AgI)x(AgPO3)1−x Glasses, Phys. Rev. Lett. 74 (1995) 726–729, doi.org/10.1103/PhysRevLett.74.726.

[66] A. Sanson, F. Rocca, C. Armellini, G. Dalba, P. Fornasini, R. Grisenti, Correlation between I-Ag distance and ionic conductivity in AgI fast-ion-conducting glasses, Phys. Rev. Lett. 101 (2008) 155901, doi.org/10.1103/PhysRevLett.101.155901.

[67] W. Meyer, H. Neldel, Uber die Beziehungen zwischen der Energiekonstanten e und der Mengenkonstanten a in der Leitwerts-Temperaturformel bei oxydischen Halbleitern, Z. Tech. Phys 18 (1937) 588–593.

[68] A. S. Nowick, W. K. Lee, H. Jain, Survey and interpretation of pre-exponentials of conductivity, J. Non-Cryst. Solids 28–30 (1988) 89–94, doi.org/10.1016/S0167-2738(88)80013-4.

[69] D. P. Almond, A. R. West, The activation entropy for transport in ionic conductors, Solid State Ionics 23 (1987) 27–35, doi.org/10.1016/0167-2738(87)90078-6.

[70] C. Liu, C. A. Angell, Mechanical vs electrical relaxation in Agl-based fast ion conducting glasses, J. Non-Cryst. Solids 83 (1986) 162–184, doi.org/10.1016/0022-3093(86)90066-9.

[71] K. L. Ngai, Meyer–Neldel rule and anti Meyer–Neldel rule of ionic conductivity: Conclusions from the coupling model, Solid State Ionics 105 (1998) 231–235, doi.org/10.1016/S0167-2738(97)00469-4.

[72] C. R. Mariappan, G. Govindaraj, B. Roling, Lithium and potassium ion conduction in $A_3TiB'P_3O_{12}$ (A=Li, K; B′=Zn, Cd) NASICON-type glasses, Solid State Ionics 176 (2005) 723–729, doi.org/10.1016/j.ssi.2004.11.008.

[73] R. A. Montani, A. Lorente, M. A. Frechero, Effect of Ag_2O on the conductive behaviour of silver vanadium tellurite glasses: Part II, Solid State Ionics 146 (2002) 323–327, doi.org/10.1016/S0167-2738(01)01023-2.

[74] R. A. Montani, S. E. Giusia, Mixed conduction of lithium vanadium tellurite glasses, Physics and chemistry of glasses 42 (2001) 12–16, http://www.ingentaconnect.com/content/sgt/pcg/2001/00000042/00000001/4201012.

[75] S. K. Ram, S. Kumar, P. R. Cabarrocas, Normal and anti Meyer–Neldel rule in conductivity of highly crystallized undoped microcrystalline silicon films, J. Non-Cryst. Solids 354 (2008) 2263–2267, doi.org/10.1016/j.jnoncrysol.2007.10.051.

[76] L. F. Mao, H. Ning, C. Hu, Z. Lu, G. Wang, Physical Modeling of Activation Energy in Organic Semiconductor Devices based on Energy and Momentum Conservations, Scientific reports 6 (2016) 24777, doi.org/10.1038/srep24777.

[77] B. Miccoli, V. Cauda, A. Bonanno, A. Sanginario, K. Bejtka, F. Bella, M. Fontana & D. Demarchi, One-dimensional ZnO/gold junction for simultaneous and versatile multisensing measurements, *Scientific reports* 6 (2016) 29763, doi:10.1038/srep29763

[78] S. Galliano, F. Bella, G. Piana, G. Giacona, G. Viscardi, C. Gerbaldi, M. Grätzel, C. Barolo, Finely tuning electrolytes and photoanodes in aqueous solar cells by experimental design, *Solar Energy* 163 (2018) 251–255, https://doi.org/10.1016/j.solener.2018.02.009

[79] F. Bella, I. Mahamed and A. Azizan, Photochemically produced quasi-linear copolymers for stable and efficient electrolytes in dye-sensitized solar cells, *J. Photochem. Photobiol. A* 289 (2014) 73–80, https://doi.org/10.1016/j.jphotochem.2014.05.018

[80] B. Andri, A. Dispas, R. M. Djang'eing'a, P. Hubert, P. Sassiat, R. Al Bakain, D. Thiébaut, J.Vial, Combination of partial least squares regression and design of experiments to model the retention of pharmaceutical compounds in supercritical fluid chromatography, *J. Chromatogr. A* 1491 (2017) 182–194, https://doi.org/10.1016/j.chroma.2017.02.030